**Supporting Information**

# What is the Role of Nb in Nickel-Rich Layered Oxide Cathodes for Lithium-Ion Batteries?

*Fengxia Xin, Hui Zhou, Yanxu Zong, Mateusz Zuba, Chen Yan, Natasha A. Chernova, Jianming Bai, Ben Pei, Anshika Goel, Jatinkumar Rana, Feng Wang, Ke An, Louis F. J. Piper, Guangwen Zhou, M. Stanley Whittingham**

Corresponding Author:

E-mail: stanwhit@gmail.com

**Keywords:** $LiNi_{0.8}Co_{0.1}Mn_{0.1}O_2$ (NMC 811); Nb coating; Nb substitution; long cycling performance

## Experimental section

**Preparation of Nb modified NMC 811.** $LiNi_{0.8}Co_{0.1}Mn_{0.1}O_2$ materials were obtained from Ecopro Company. Niobium ethoxide (Sigma Aldrich) was used as precursor. Ecopro NMC 811 powders were mixed with niobium ethoxide in a flask and ethanol was added to the mixture. They were stirred overnight, then ethanol was evaporated at 80 °C. Pristine NMC 811, 0.7% and 1.4%, 2.1% and 3.5% Nb (molar ratio) modified NMC 811 were sintered in pure oxygen atmosphere for 3 h from 400 to 800 °C and cooled down with a cooling rate of 5.0 °C/min. Here we denote 0.7%Nb modified NMC 811 heated from 400 to 800°C as NMC811-0.7Nb-400°C, NMC811-0.7Nb-500°C, NMC811-0.7Nb- 600°C, NMC811-0.7Nb-700°C and NMC811-0.7Nb-800°C. However, we need to mention that those high temperature treatment samples are no longer NMC 811 due to Nb modification.

**Structural Characterization.** X-ray powder diffraction (XRD) patterns of 0.7% Nb modified NMC 811 samples heated in different temperature was scanned with a BRUKER diffractometer (D8 Advance) equipped with Cu $K_\alpha$ source ($\lambda$ = 1.54178 Å) with spinning. The synchrotron XRD pattern of pristine NMC 811 and 1.4% Nb modified NMC 811 were performed at sector 28−ID−2 of National Synchrotron Light Source II (NSLS-II) at Brookhaven National Laboratory. The wavelength of the X-ray was 0.18266 Å. The neutron diffraction (ND) patterns of the pure NMC 811 and the Nb modified NMC 811 samples were measured at the VULCAN instrument[1], at the Spallation Neutron Source, Oak Ridge National Laboratory. The neutron data were processed using VDRIVE software[2], and Rietveld refinement was carried out using GSAS software and

EXPGUI interface[3-4] to calculate the phase fractions, lattice parameters and site occupancy fractions. X-ray Photoemission Spectroscopy (XPS) was performed using a Phi VersaProbe 5000 system with a monochromated Al Kα source and hemispherical analyzer at the Analytical and Diagnostics Laboratory (ADL) at Binghamton University. All samples were mixed with graphite to be used as reference. The core-levels (O 1s, Ni 2p, Nb 3d) were measured with a pass energy of 23.5 eV, corresponding to an instrumental resolution of 0.5 eV from analyzing both the Au 4f7/2 and Fermi edge of the Au foil. A flood gun was used to neutralize any charge build up during measurements. Samples for X-ray absorption near edge structure (XANES) and Extended X-ray absorption fine structure (EXAFS) were prepared by mixing ~ 10 mg of materials with graphite and pressed in the form of pellets. Nb K-edge XANES and EXAFS for 0.7% Nb modified NMC 811 samples heated from 400 to 800 $^{o}$C were tested using a fluorescence detector and calibrated using Nb reference foil in beamline 20 BM in Advanced Photon Source, Argonne National Lab. The samples morphology was determined using a Zeiss SUPRA 55 VP field emission scanning electron microscopy (SEM) at an operating voltage of 5 kV. High-angle annular dark-field (HAADF) scanning transition electron microscopy (STEM), energy-dispersive X-ray spectroscopy (EDS), High resolution transition electron microscopy (HR-TEM) images were collected using a FEI Talos F200X (200 keV) at the Center for Functional Nanomaterials in Brookhaven National Lab. The magnetic properties were tested by a Quantum Design SQUID magnetometer (MPMS XL-5). Field-cooled (FC) and zero-field-cooled (ZFC) magnetizations were measured from 298 to 2 K in magnetic fields of 10 Oe. The thermal stability tests were performed via differential scanning calorimetry (DSC) (Q200, TA) at a scan rate of 2.5 °C/min.

The test cathodes were charged to 4.4V versus lithium in 2032-type coin cells and disassembled in the glovebox. After washing with dimethyl carbonate (DMC) to remove the residues, the electrode was cut into a small piece of 5 mg and sealed in a gold-capped stainless-steel crucible with 3 μL electrolyte (1M $LiPF_6$ in EC/DMC) to do the DSC test.

**Electrochemical measurement.** Nb modified NMC 811, heated from 400 to 800 °C and pristine NMC 811 samples were mixed with acetylene black and polyvinylidene fluoride (PVDF) powders with a weight ratio of 90:5:5 in 1-methyl-2- pyrrolidinone (NMP) solvent to form a slurry. Then the slurry was cast onto an aluminum (Al) foil using doctor blade and dried in vacuum oven at 80 °C for overnight. The average mass loading of the electrode was 13-15 $mg/cm^2$ and was calendared to 3.0 $g/cm^3$. All of this was done in our dry room (Temperature: 20-21 °C; Dew point: < -50). For the coin cells, Li foil was used as a counter/reference electrode, a Celgard 3501 membrane as a separator and 1.0 M $LiPF_6$ dissolved in ethylene carbonate/dimethyl carbonate (EC/DMC, 1:1 in volume) as the electrolyte solution. For the first cycle test of the electrode, a current density of C/10 (1 C = 200 mAh/g) was used between 2.8 and 4.6 V. Different rate performance (C/10, C/5, C/2, C, and 2C) was also tested. The cycling was set in the current density of C/3 charge and C/3 discharge. For long cycling, we set 2.8 to 4.4 V for the first two cycles in the current density of C/10, then C/10 charge, hold at 4.4 V for 1h or the current drop down to C/60 and C/3 discharge for the following cycles. These data were obtained on a multichannel Biologic system.

**Reference**

(1) An, K.; Skorpenske, H. D.; Stoica, A. D.; Ma, D.; Wang, X.-L.; Cakmak, E. First in situ Lattice Strains Measurements under Load at VULCAN. *Metall. Mater. Trans.* **2011,** *42*, 95-99.

(2) An, K. VDRIVE-Data reduction and Interactive Visualization Software for Event Mode Neutron Diffraction. *ORNL Report No. ORNL-TM-2012-621* **2012**.

(3) Larson, A.; Von Dreele, R. General Structure Analysis System (GSAS)(Report LAUR 86-748). *Report LAUR 86-748* **2004**.

(4) Toby, B. H. EXPGUI, a Graphical User Interface for GSAS. *J. Appl. Crystallogr.* **2001,** *34*, 210-213.

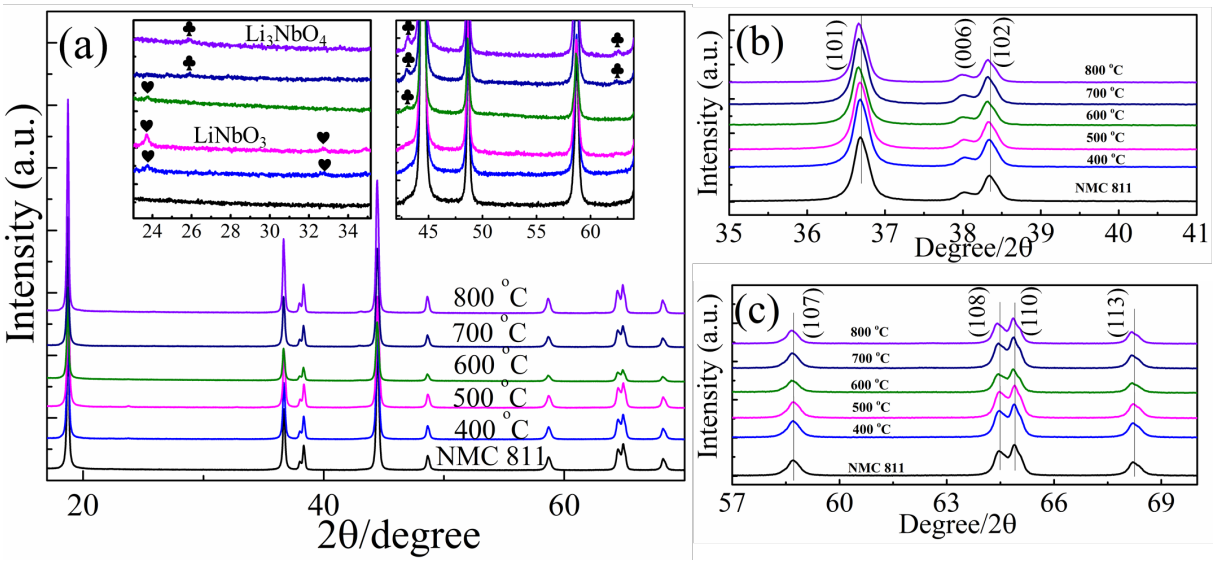


**Figure S1.** (a) XRD patterns of 0.7% Nb modified NMC 811 heated at different temperatures. Inset shows impurity peak, ♥ is $LiNbO_3$ and ♣ is $Li_3NbO_4$; (b) and (c) Enlarged view in 2θ degree.

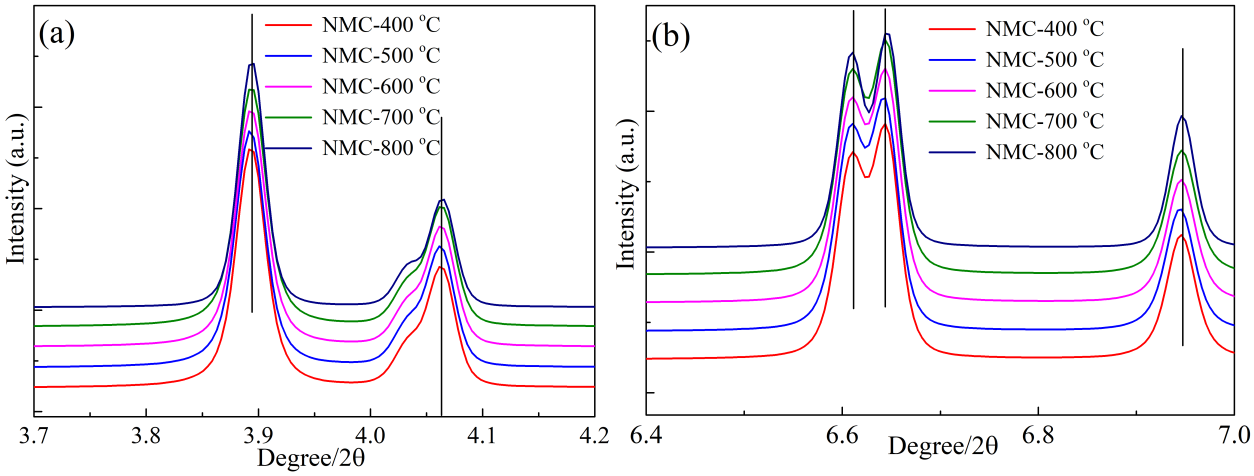


**Figure S2** (a) and (b) Enlarged synchrotron XRD patterns of market NMC 811 heated at different temperature from 400 to 800 °C.

**Table S1.** Refined lattice parameters for 1.4% Nb modified NMC 811 heated from 400 to 800 °C.

| T, °C | a, Å | c, Å | V, Å$^3$ | c/a | $R_{wp}$, % |
|---|---|---|---|---|---|
| 400 | 2.8746(1) | 14.198(1) | 101.60(1) | 4.939 | 9.2 |
| 500 | 2.8752(1) | 14.199(1) | 101.66(1) | 4.938 | 10 |
| 600 | 2.8759(1) | 14.202(1) | 101.73(1) | 4.938 | 9.5 |
| 700 | 2.8763(1) | 14.204(1) | 101.77(1) | 4.938 | 9.7 |
| 800 | 2.8778(1) | 14.210(1) | 101.92(1) | 4.938 | 8.7 |

**Table S2.** Refined lattice parameters for commercial NMC 811 heated from 400 to 800 °C.

| T, °C | a, Å | c, Å | V, Å$^3$ | c/a | $R_{wp}$, % |
|---|---|---|---|---|---|
| 400 | 2.8745(1) | 14.197(1) | 101.59(1) | 4.939 | 8.9 |
| 500 | 2.8750(1) | 14.198(1) | 101.64(1) | 4.938 | 9.3 |
| 600 | 2.8744(1) | 14.198(1) | 101.59(1) | 4.939 | 9.2 |
| 700 | 2.8742(1) | 14.197(1) | 101.57(1) | 4.939 | 8.9 |
| 800 | 2.8738(1) | 14.197(1) | 101.54(1) | 4.940 | 8.8 |

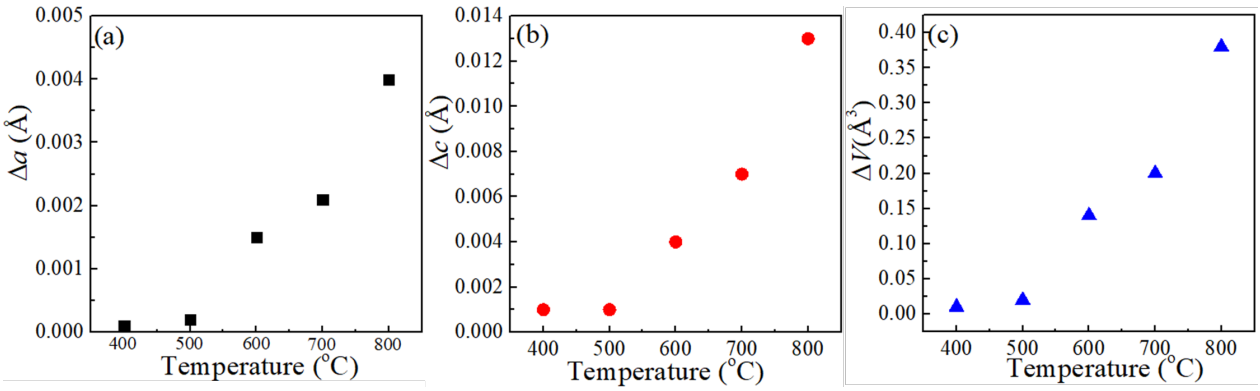


**Figure S3**. Increase lattice parameters in 1.4% Nb modified NMC 811 heated from 400 to 800 °C compared with pure NMC 811, based on **Table S1** and **Table S2**.

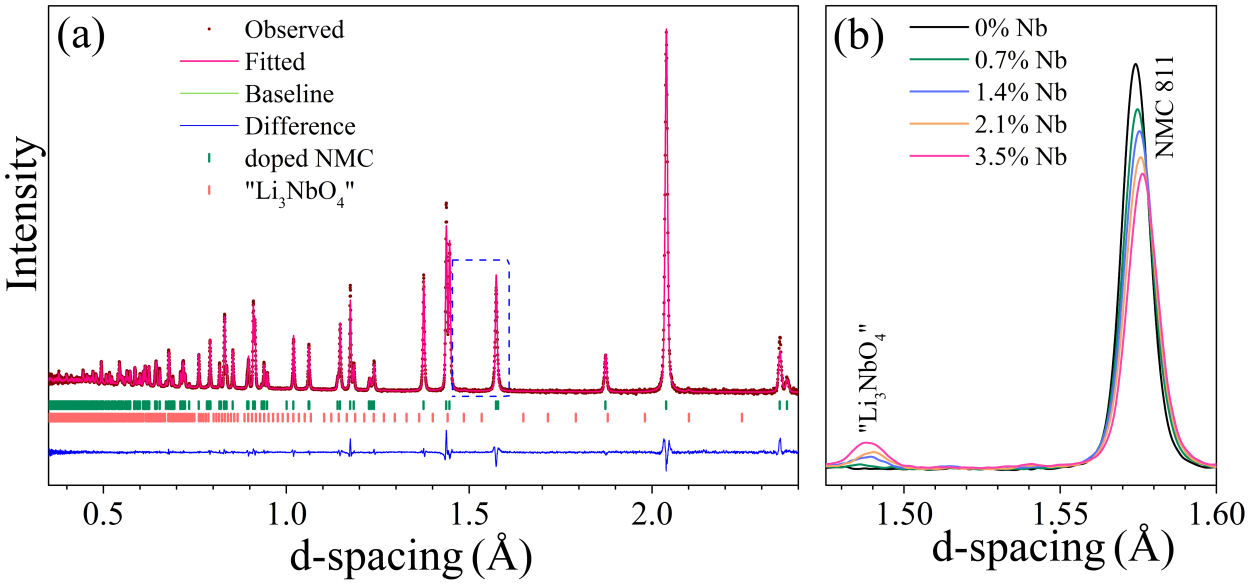


**Figure S4**. (a) The high-resolution neutron diffraction pattern along with Rietveld refinement of 0.7% Nb modified NMC 811, and (b) the magnified view of the region with dashed rectangle showing the evolution of the characteristic peaks of NMC 811 and the precipitate "$Li_3NbO_4$" upon different amounts of Nb modification sintered at 800 °C

**Table S3**. The neutron coherent scattering lengths and the ion radii of selected elements. (LS – low spin; HS – high spin)

| Elements | Neutron coherent scattering length (fm) | Ion radii at 6-coordination (Å) |
|---|---|---|
| Ni | 10.3 | 0.48($Ni^{4+}$); 0.6 ($Ni^{3+}$,HS); 0.56 ($Ni^{3+}$,LS); 0.69($Ni^{2+}$); |
| Mn | -3.73 | 0.53 ($Mn^{4+}$); 0.645 ($Mn^{3+}$,HS); 0.58 ($Mn^{3+}$,LS); 0.83 ($Mn^{2+}$,HS); 0.67 ($Mn^{2+}$,LS) |
| Co | 2.49 | 0.53 ($Co^{4+}$); 0.61 ($Co^{3+}$,HS); 0.545 ($Co^{3+}$,LS); 0.745 ($Co^{2+}$,HS); 0.65 ($Co^{2+}$,LS) |
| Nb | 7.054 | 0.64 ($Nb^{5+}$) |
| Li | -1.9 | 0.76 ($Li^{+}$) |

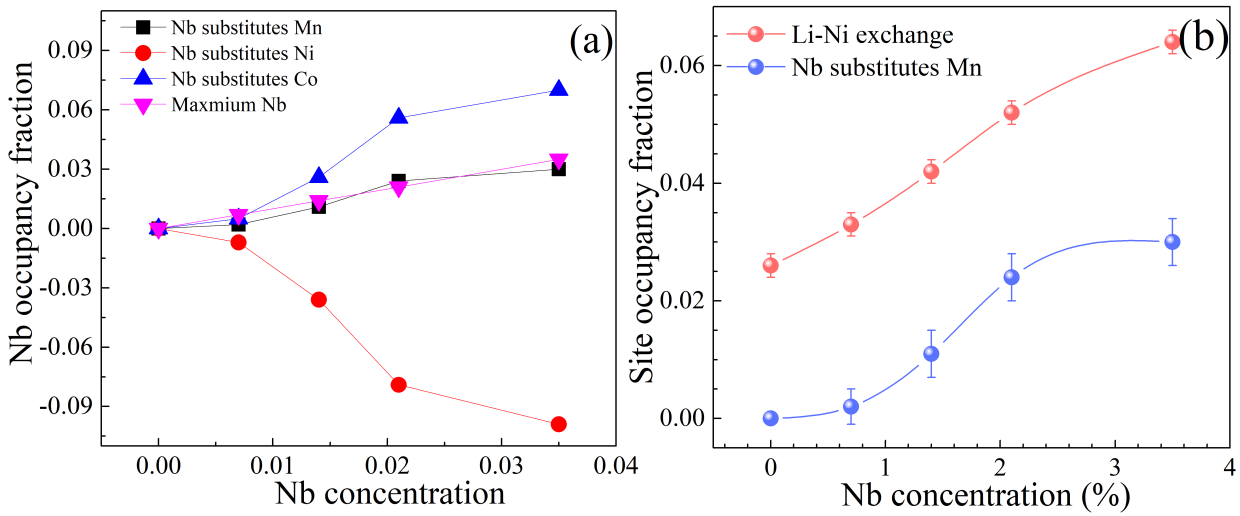


**Figure S5**. (a) The refined Nb occupancy fraction when Nb substitutes Mn, Ni or Co in NMC 811; (b) The Li-Ni exchanging between Li-site and TM-site are promoted by Nb modification with a nearly linear dependence while Nb substituting Mn at TM-site increases under a nonlinear trend.

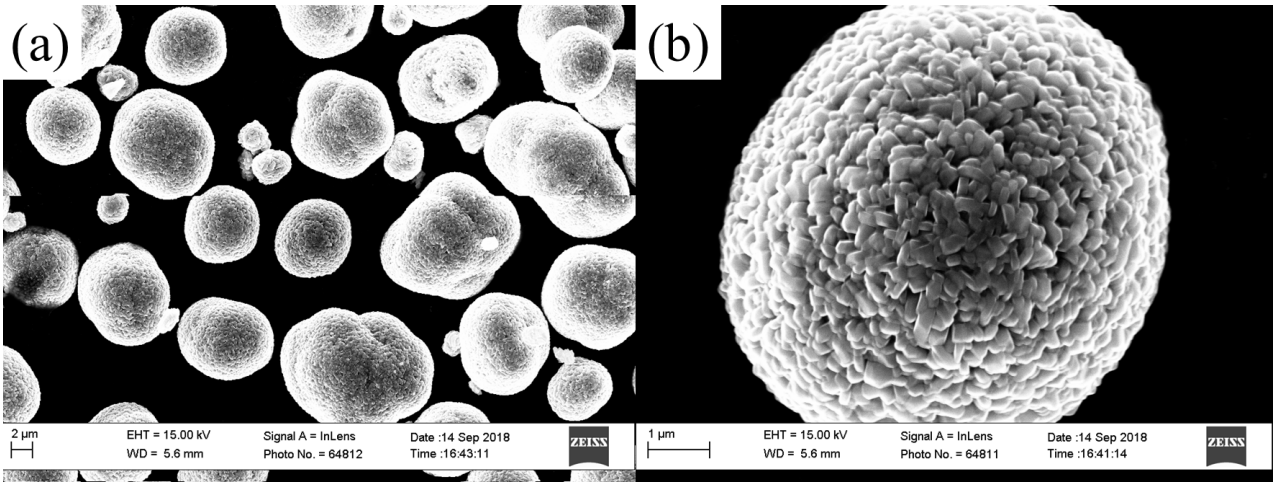


**Figure S6.** SEM images of pure NMC 811.

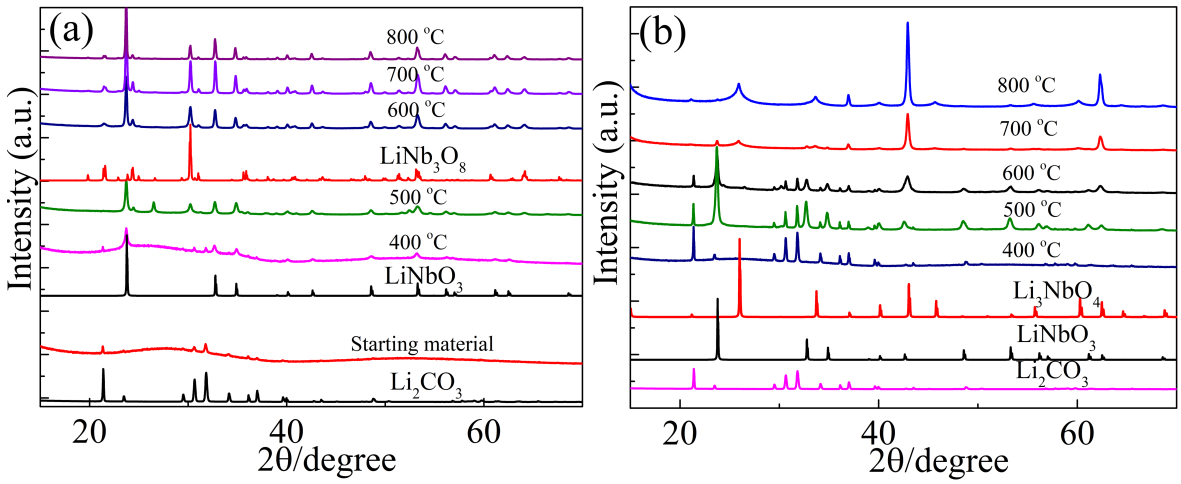


**Figure S7** XRD patterns of Nb compound and $Li_2CO_3$ mixed with a molar ratio 1:0.5 (a) and 1:1.5 (b) and sintered from 400 to 800 °C for 3 h in $O_2$.

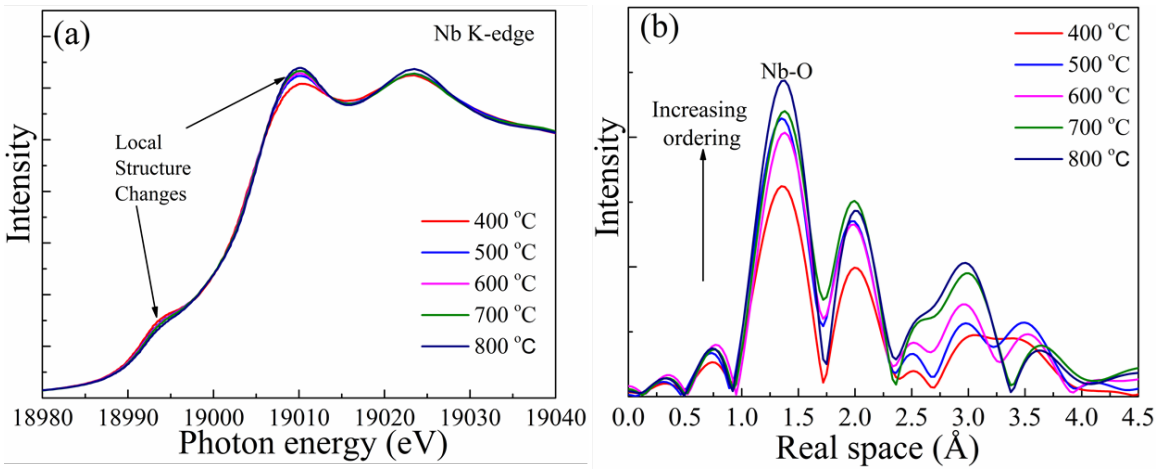


**Figure S8**. (a) Nb K-edge XANES and (b) EXAFS of 0.7% Nb modified NMC 811.

**Magnetic Susceptibility Study**

Valence information for pristine NMC 811 and Nb modified NMC 811 samples was investigated by magnetic susceptibility tests. **Figure S9 (a)** presents field-cooled (FC) and zero-field-cooled (ZFC) susceptibilities of 0.7% Nb modified samples treated at various temperatures from 400 to 800 °C in comparison with that of NMC 811 sample. In NMC 811, the temperature dependence of the magnetic susceptibility follows the Curie-Weiss law at high temperatures, where FC and ZFC curves closely match each other. The Curie-Weiss law fitting parameters presented in **Table S4**, show excellent match between the experimental effective moment, and that calculated assuming 0.1 $Co^{3+}$ (S=0), 0.1 $Mn^{4+}$ (S=3/2), 0.1 $Ni^{2+}$ (S=1), and 0.7 $Ni^{3+}$ (S=1/2). At 10.0 K a magnetic transition is observed, below which FC and ZFC curves depart in NMC 811 samples. For Nb modified NMC 811 samples, the transition temperature does not change in samples heated at 400 and 500 °C, while in the samples heated at higher temperatures (600 °C, 700 °C and 800 °C), the magnetic transition shifts to 11.5 K (**Figure S9b**). The increase in the transition temperature at higher treatment temperatures further confirms lattice modification by Nb substitution, which should lead to the change in the transition metal oxidation states. However, the experimental effective magnetic moment shows no or little change in higher-temperature Nb-treated NMC 811, which may be explained by the low Nb substitution level (0.7%).

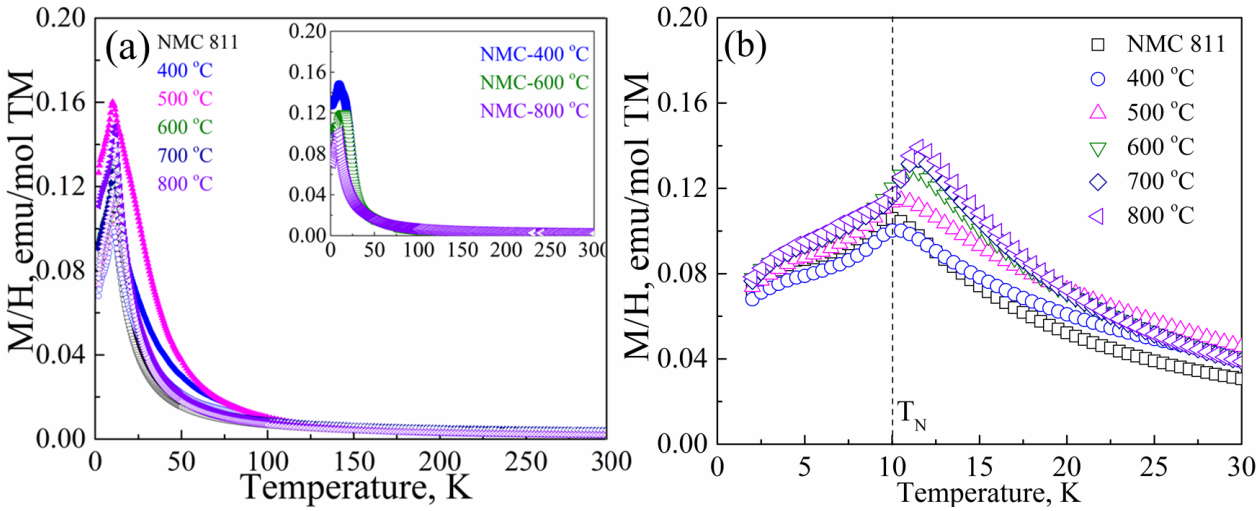


**Figure S9**. (a) Field cooled (solid symbols) and zero-field cooled (open symbols) of Nb-O modified 811 samples and pure NMC sintered at 400, 600 and 800 °C. (b) Magnified view of zero-field cooled (ZFC) susceptibilities near the ordering transitions of Nb-O modified 811 samples. Inset shows ZFC of pure NMC sintered in 400 °C, 600 °C and 800 °C.

**Table S4**. Magnetic parameters of Nb modified NMC 811 and pure NMC 811 in different temperature.

| Sample | $C_M$, emu K/ mol TM | $\Theta$, K | $\chi_0$, $10^{-4}$ emu/mol TM | $T_f$, K | $\mu_{exp}$, $\mu_B$ | $\mu_{theor}$ $Ni2+$ $Mn4+$, $\mu_B$ |
|---|---|---|---|---|---|---|
| NMC 811 | 0.565(1) | 10.8(1) | 1.1 | 10.0 | 2.13 | 2.10 |
| 0.7% Nb-400 °C | 0.459 | 31.3 | -1.5 | 10.0 | 1.92 | 2.10 |
| 0.7% Nb-500 °C | 0.532 | 17.6 | 1.7 | 10.5 | 2.06 | 2.10 |
| 0.7% Nb-600 °C | 0.577 | 13.3(1) | 6.7 | 11.0 | 2.15 | 2.10 |
| 0.7% Nb-700 °C | 0.518 | 17.4(1) | 13.1 | 11.5 | 2.04 | 2.10 |
| 0.7% Nb-800 °C | 0.532 | 18.2(1) | 1.8 | 11.5 | 2.06 | 2.10 |
| NMC-400°C | 0.566 | 9.2 | 1.5 | 10.0 | 2.13 | 2.10 |
| NMC-600°C | 0.563 | 7.1 | 0.9 | 9.5 | 2.12 | 2.10 |
| NMC-800°C | 0.588 | 3.6 | 0.07 | 9.5 | 2.17 | 2.10 |

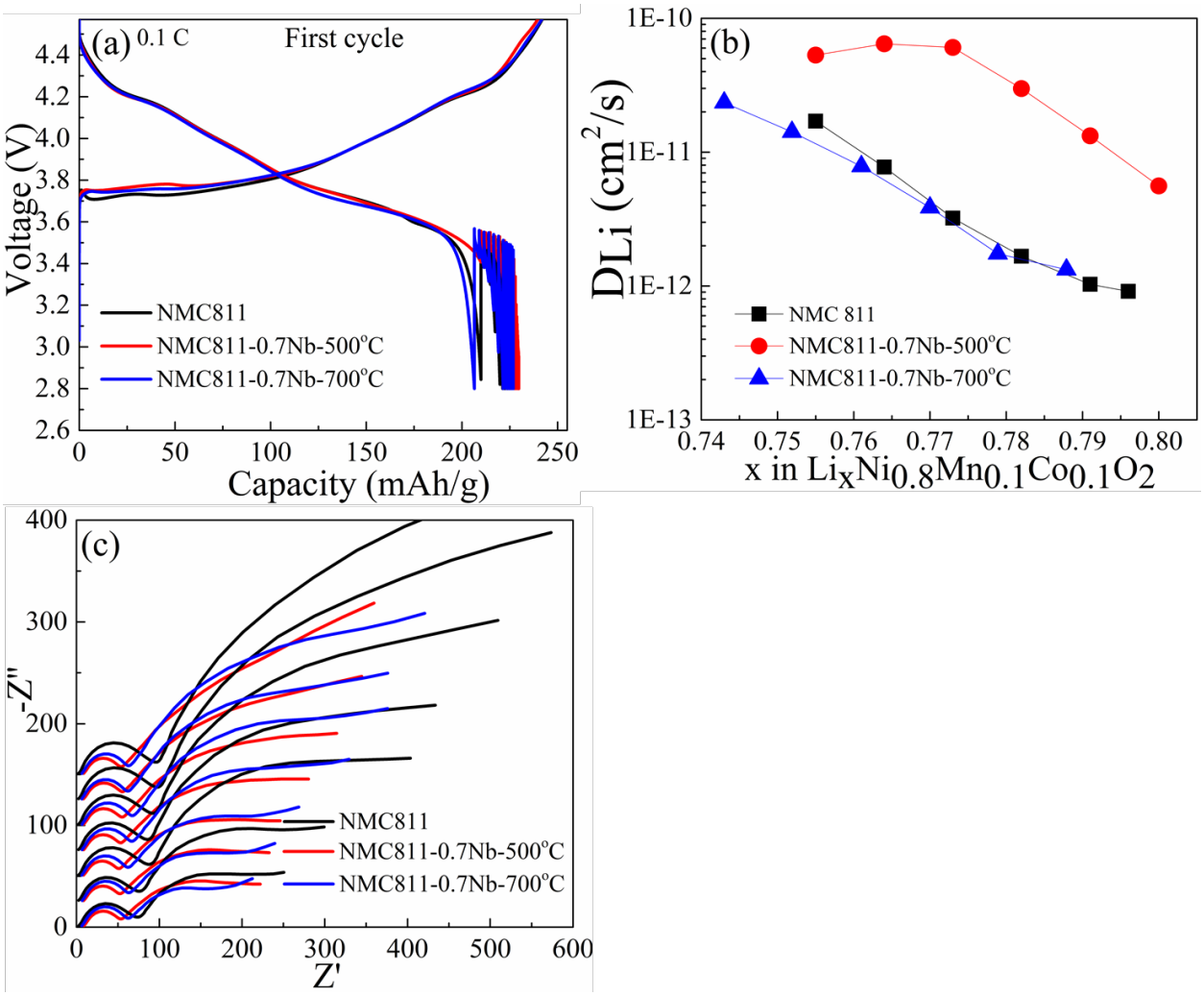


**Figure S10**. (a) GITT curves in lower voltage range of discharge process; (b) calculated lithium-ion diffusion coefficients; (c) EIS (in lower voltage range of discharge process) of Nb modified NMC 811 at 500 °C, 700 °C and pure NMC 811.

**Thermal Stability Study**

**Figure S11** shows the large exothermic peaks shifts from 199.4 ℃ (NMC 811) to 203.7 ℃ (Nb modified NMC 811 heated at 500 ℃) and 204.3 ℃ (Nb modified NMC 811 heated at 700 ℃) although an additional peak starts from 143.1 ℃ for the 700 ºC sample. The heat release amounts are 203.9 J/g (NMC 811) vs. 174.6 J/g (Nb modified NMC 811 heated at 500 ℃) vs.161.72 J/g (three peaks: 28.60+58.89+78.23J/g in 700 ℃ sample).

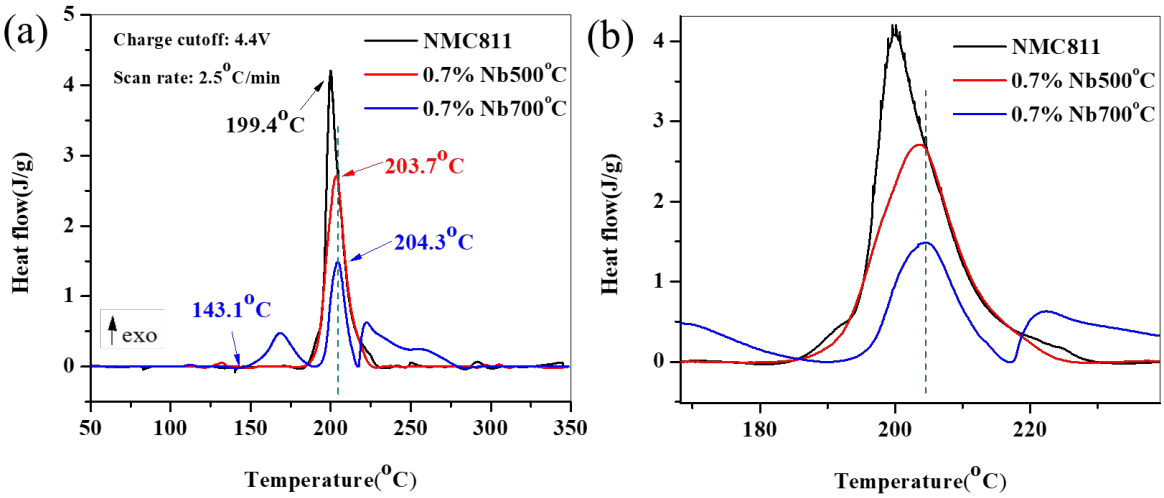


**Figure S11**. DSC profiles of NMC 811 and Nb modified NMC 811 heated at 500 ℃ and 700 ℃ charged at 4.4 V vs. Li+/Li.